Chapter 7.2

DIGITAL IMAGE ANALYSIS CONTRIBUTION TO THE EVALUATION OF THE MECHANICAL DECAY OF GRANITIC STONES AFFECTED BY FIRES

Miguel Gómez-Heras[1], Carlos Figueiredo[2], María José Varas[1], Antonio Maurício[2], Mónica Álvarez de Buergo[1], Luis Aires-Barros[2], Rafael Fort[1]
[1]Instituto de Geología Económica (CSIC-UCM), C/ José Antonio Novais 2. Facultad de CC. Geológicas, Universidad Complutense. 28040 Madrid, Spain; [2]Centro de Petrología e Geoquímica do Instituto Superior Técnico. Av. Rovisco Pais 1049-001 Lisboa, Portugal

Abstract: The study of the decay promoted in building stones by fire is important in the context of the conservation and restoration of historic buildings. As opposed to granular stones, which are more sensitive to chemical changes, tough stones present a noticeable mechanical decay after being affected by fires. The direct observation of decay features at a micro-scale could be the key for understanding the decay processes at greater scales, especially in the cases where extensive sampling is not recommendable or even possible. Microscopic techniques allow quantifying fracture system and establishing differences among different types of fractures. Results obtained so far have demonstrated image analysis and processing techniques as a useful tool to help establishing, in a qualitative and quantitative way, the fracture system variations resulting from mechanical stresses induced by fire.

Key words: granitic stones; stone decay; thermal behaviour; petrophysics; fracture systems; image analyses.

1. INTRODUCTION

Fire is a significant decay agent of stone-made historic buildings, as the temperature gradients generated during and after fire can be enough to promote a short-term irreversible decay in building stones. Moreover, it is thought that fire causes the damage of about one historic building in the European Union each day (COST C17, 2001).

S.K. Kourkoulis (ed.), Fracture and Failure of Natural Building Stones, 427–437.

Fire may generate both chemical and physical changes in building stones. The type and intensity of these damages will depend mainly on the temperatures attained and, specially, of the type of burnt material (Gómez-Heras, 2006). Granular stones are more sensitive to chemical changes while tough and dense stones present a noticeable mechanical decay after being affected by fires. Mechanical decay consists mainly of the generation or growth of fissures due to the thermal stresses. Studies on burnt stones had focused the attention to the bulk mechanical changes (Allison and Goudie, 1994; Chakrabarti et al., 1996), whose testing is relatively sample-costly. This is not in consonance with the sampling of heritage buildings that must try to deal with samples as inconspicuous as possible. In the last years, this trend has shifted to the observation of variations at a more detailed scale, that is to asses mineralogical and micro-morphological changes (Ehling and Kohler, 2000; Hajpál, 2002; Gómez-Heras et al., 2004; Hajpál and Török, 2004; Gómez-Heras, 2006).

The direct observation of decay features at a micro-scale shall be a key for understanding the processes at greater scales both in terms of space (i.e. fracture mechanisms and patterns within the stone) and of time (i.e. future physical behaviour of the stone). Microscopic techniques allow quantifying the fracture system and establishing differences among different types of fractures according to Griffith fracturing criteria. Microscopic techniques have also the advantage of being compatible with small amounts of destructive sampling. These techniques at the micro-scale are complementary to direct and indirect bulk dynamic testing, that enable to compare the 'quality' of bigger samples of stone before and after fires.

Image analysis is both a low-cost and easy to handle non-destructive methodology that is suitable for the assessment of building stone decay (Mauricio and Figueiredo, 2000). Several papers concerning the use of digital image processing and analysis techniques in field and laboratory studies in order to contribute to an accurate assessment of environment-induced damage could, for instance, be referred: Aires-Barros et al. (1991); Ortiz et al. (2000); Zezza (1989).

In this research, some numerical parameters and indexes are proposed to evaluate the mechanical state of the rock at the micro-scale. These numerical indexes are based on different parameters such as fracture length/perimeter area, density or orientation, obtained after refining the images by applying some linear filters and morphological processing techniques for fractures and grain joints detection.

2. MATERIALS AND METHODS

Samples of granite that had been burnt by limited bonfires in two different historic buildings were studied. These buildings are placed in rural areas within the region of Madrid: The *Coracera* Castle (14^{th}–15^{th} century,

San Martín de Valdeiglesias, Madrid) and the *Infante Don Luis* Palace (18th century, Boadilla del Monte, Madrid). Fire temperature was estimated in around 500 ºC due to the mineralogical changes found (Gómez-Heras, 2006).

The granitic stones from the Guadarrama's mountain range (which is located in the north part of the region of Madrid, Spain) are the most important building stone types in the central area of the Iberian Peninsula. These types of granitic stones have been historically included within the term *Piedra Berroqueña*, which include compositions from leucogranites to granodiorites and monzogranites.

Two samples of about 30 cm^3 were taken for the microscopic evaluation. Samples were impregnated with an epoxy resin containing fluorescent dye and cut perpendicular to the burnt surface. Two thin sections were made from each sample, both comprising the external burnt area and the internal area unaffected by the fire. The unaffected portion of the rock was considered as the standard to compare the microcrack pattern before and after the fire.

Sample images in colour RGB (for Red, Green and Blue colour component) format of fracture patterns of the granite samples were acquired using Oxford Inca 4.09 software coupled to a JEOL JSM 6400 Scanning Electron Microscopy (SEM) in Secondary and Backscatter Electrons modes and with a 3.34 million pixel resolution. DP12-BSW *Olympus* Camera connected to an *Olympus* Polarizing Microscope coupled with an *U-RFL-T* Ultraviolet Fluorescence Microscopy unit. *Olympus DP-Soft* v. 3.2 was used for image acquisition. Several of these colour digital images, with different size ranging from 994x744 to 1024x768 pixels, were then processed for quantitative analysis of the fracture system patterns. Four types of images were used for the image analysis depending on the acquisition media: Polarizing Microscope, Fluorescence Microscope and Scanning Electron Microscope (Secondary and Backscattered electrons modes)

Starting with the initial RGB images, processing has typically involved the conversion of these images to the HLS format (composed of components representing the hue, luminance and saturation). Techniques for enhancing contrast, noise removing and segmentation into binary images of the resulting grey level (intensity) images were also used.

Dealing with several images and each one having specific characteristics, the processing step has used a casuistic/task-oriented approach. For a thorough illustration of the image processing performed in this work two step-by-step examples of image processing and analysis are provided. Several operations were sequentially accomplished to perform the complete chain of image processing. Some of the most common operations applied in this study will then be presented in the following steps:

- **preprocessing:** grey level images (Figures 1a, 2a), more suitable to this dedicated application and representing only the intensity component (L), were obtained from the conversion of the initial colour RGB images to

the HLS colour format, encoded as Hue, Lightness and Saturation (Gonzalez and Woods, 1993).

- **filtering:** different techniques have been used depending on the task/ purpose. *Opening* transforms (Coster and Chermant, 1985; Mauricio and Figueiredo, 2000; Serra, 1982) of the grey-scale images coming from the preprocessing, were, sometimes, performed for noise (small light details) removing and contrast enhancing (Figure 1b); *hole-fill* (Figure 2c), a classical, sophisticated and complex morphological algorithm has also been used, in some cases, on the background of binary images derived from the segmentation of grey level images, for removing small features (which are mostly noise in the image), and leaving a more statistically significant sampling of fracture system pattern and improving its detection in the cleaned final image (Figure 2d).
- **segmentation:** the grey level images (previously enhanced or not) were segmented into binary images for fracture patterns extraction and individualization from the background, performing either a *thresholding algorithm* (Figure 2b) or the so called morphological *black top-hat* transform (Figure 1c), to detect the dark area of the image**.** Another sophisticated algorithm combining a *thresholding* transformation with the *skiz* (the skeleton by zone of influence) of the back ground was also used to detect the fracture pattern in some particular images as shown in Figure 1d.
- **arithmetic** and **logical operations:** some of these operations were performed either on binary images during the processing chain procedure or to generate the final composed images (Figures 1e, 2d) obtained from the initial grey level images and the final refined and segmented binary images of fracture system patterns.

On the refined and segmented binary images previously derived from the image processing step, different types of parameters such as fracture length/ perimeter, area, density and orientation, were then obtained using basic formulae (Aires-Barros et al., 1991; Coster and Chermant, 1985; Figueiredo et al., 1993; Serra, 1982):

- The area measure (A (X)) returns, on a binary image (X), the number of non zero pixels in the image. If the image is calibrated, the area in pixels is scaled to give the area in the measurement unit (mm^2) associated with the image. The sample (A(S)) and fracture system pattern (A(fs)) areas were then estimated.
- The *perimeter* measure (L(X)) (mm) designates the length of the object boundary. It was estimated using the *Crofton* formula. For closed fracture system pattern, one pixel width, its *length* (*L(fs)*) was computed.
- The *rose of directions***,** characterizing the directional structure of contours or line sets, is a powerful theoretical tool to point the major directions of an object (Figure 1f). It is the density of the contour length as a function of the tangent direction.

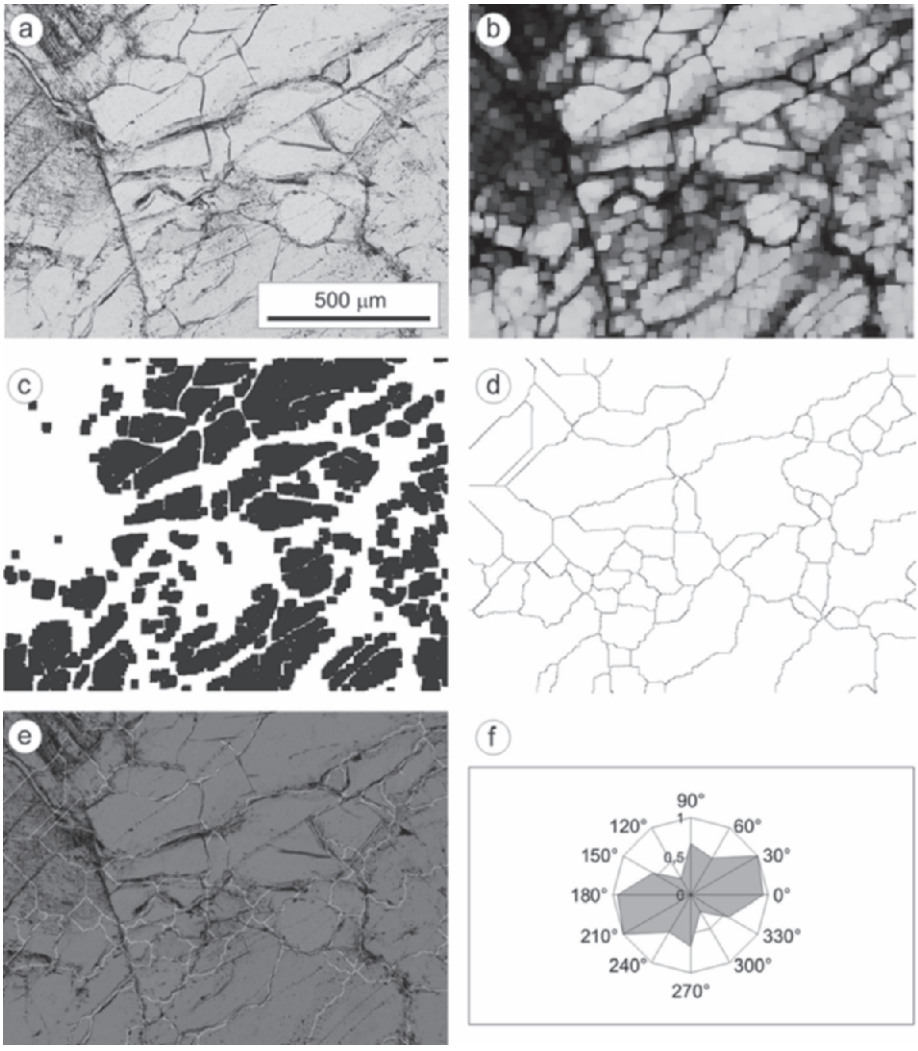

Figure 1. (a): Original image obtained with polarizing microscope (parallel nicols): grey level image; (b): Result of an opening performed on the image (a); (c): Binary image obtained by performing a "black top-hat" transform on the image (b); (d): Result of performing a "skiz" transform on the background of the image (c); (e) Composite image obtained by combining the original image a and the refined, cleaned and simplified binary image (d). The different fracture types could be identified in this image. (f): Rose of directions diagram for the whole fracture system pattern detected on the original image.

Based on some of these basic parameters additional ones were estimated, such as the roughness index (*RI (fs) = L(fs)/ A(fs)*) (useful for the distinction between *open* (RI< 1) and *closed* (RI=1) fracture system pattern, and where *L(fs)* and *A(fs)* are estimated in pixels) (Aires-Barros et al., 1994)**,** the *specific surface area***,** ($A_A(fs)$) (%)**,** and the *specific perimeter/length* ($L_A(fs)$) (mm^{-1}).

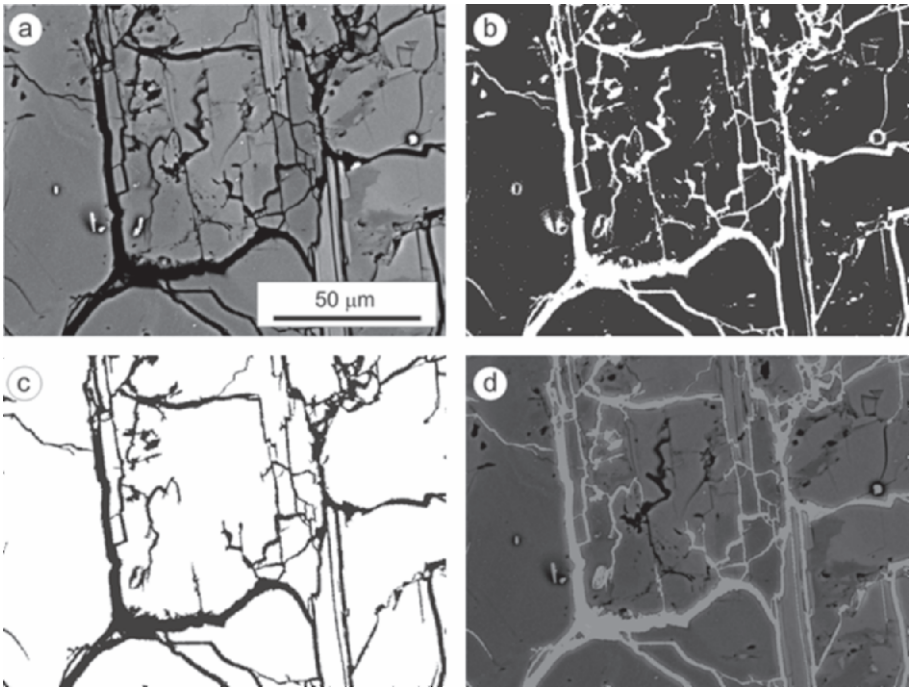

Figure 2. (a): Original image: grey level image; (b): Binary image obtained by thresholding of image (a); (c): Result of performing a "hole-fill" transform on the background of the image (b); (d): Composite image obtained by combining the original image (a) and the refined, cleaned and simplified binary image (c). The different fracture types can be identified in this image.

3. RESULTS

The samples of granite showed macroscopically in all cases a surface discolouration due to a fine deposit of ashes and a slight reddening affecting the first few millimetres of stone. No major fissures are detected macroscopically. The petrographic observations of the selected samples correspond with a fine to medium grained panalotriomorphic equigranular leucogranite. Principal minerals are quartz, plagioclase and potassium feldspar. Accessory minerals are biotite and apatite. Feldspar is generally sericitized and presents abundant pertitic textures.

The microscopic observation of thin sections of this granite shows that the outer portion of stone is much more fissured than the internal areas not affected directly by fire. The most noticeable fissures are sub-parallel to the burnt surface. Individual crystals present an intense internal fissuration in the external burnt area. This is especially noticeable in feldspars (both plagioclases and K-feldspars). Weak surfaces, such as exfoliation planes, altered areas (sericitized feldspars) or inclusions favour the fissuration.

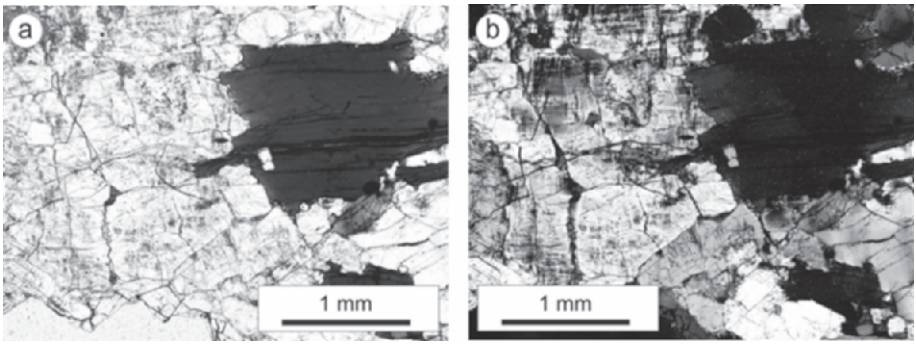

Figure 3. Photomicrographies of leucogranite samples from *Infante Don Luis* Palace. Parallel (a) and crossed (b) nicols.

Fluorescence Microscopy shows the existence of three types of fissures in the material: intergranular fissures (in the interface of two mineral grains), intragranular (breaking single mineral grains), and transgranular (a combination of the previous fissures). SEM images reveal that in the most external zones (0.5 cm deep from the surface) the three types of fissures are present (inter, intra and transgranular). Towards the interior of the stone sample (deeper than 0.5 cm from the surface), transgranular fissures disappear, and deeper, the intragranular ones disappear also (1 cm deep from the surface). There are no fire-induced fissures above 1.5 cm deep from the exposed surface of the samples. A set of analysis was then performed on a number of binary images, and statistics of some parameters and indexes on the measures performed are given in Table 1.

Table 1. Some basic statistics of the parameters measured on the Fracture System Pattern in 'fresh' and burnt samples

		A(S) (mm^2)	A(fs) (mm^2)	A_A(fs) (%)	L(fs) (mm)	L_A(fs) (mm^{-1})	RI(fs)
'Fresh' areas	**Minimum**	8.67	0.18	2.07	85.03	9.81	1.00
	Maximum	8.67	0.29	3.36	137.63	15.87	1.00
	Average	**8.67**	**0.24**	**2.71**	**111.33**	**12.84**	**1.00**
	St. Deviation	0.00	0.08	0.91	37.19	4.29	0.00
		A(S) (mm^2)	**A(fs) (mm^2)**	**A_A(fs) (%)**	**L(fs) (mm)**	**L_A(fs) (mm^{-1})**	**RI(fs)**
Burnt areas	**Minimum**	0.02	0.00	0.91	0.89	10.24	0.17
	Maximum	8.67	0.21	16.30	88.81	441.07	1.00
	Average	**0.98**	**0.04**	**8.60**	**23.00**	**123.39**	**0.52**
	St. Deviation	2.12	0.07	5.43	22.79	142.42	0.32

Symbols in Table 1 are as follows: A(S) is the area of the sample; A(fs) is the area of the Fracture System pattern; A_A(fs) is the specific surface area of Fracture System pattern; L(fs) is the perimeter/length of the Fracture System pattern; L_A(fs) is the specific perimeter/length of the Fracture System pattern and finally RI(fs) is the Roughness Index.

The calculated parameters (specific surface area A_A(fs), specific length L_A(fs) and roughness index RI(fs)) are the best for establishing the comparison between burnt and non-burnt areas of the studied stone: surface area in the burnt areas is about four times greater than in non-burnt areas. More evident is the increase in the specific length of fissures, which reaches values up to more than twenty times greater than the values obtained in non-burnt areas. Average roughness index decreases from the value RI = 1, which represent a totally 'closed' fracture system pattern to 0.52.

Regarding the orientation of fissures (Figure 4), burnt areas show a main direction of fissures parallel to the burnt surface. A second system of fissures appears perpendicularly or sub-perpendicularly in much smaller proportion. The closer to the burnt surface the more abundant are these perpendicular fissures.

The fissuration perpendicular to the surface has two origins; firstly the occurrence of fissures conjugated with the fissures parallel to the surface. Secondly, intergranular unions are more likely to open in the surface grains. The strain undergone by the minerals during a fire is proportional to the temperature distribution within the rock, which decrease exponentially inwards.

Relative proportion of inter-, intragranular fissures varies between burnt and non-burnt areas. Non-burnt areas present a homogeneous proportion of

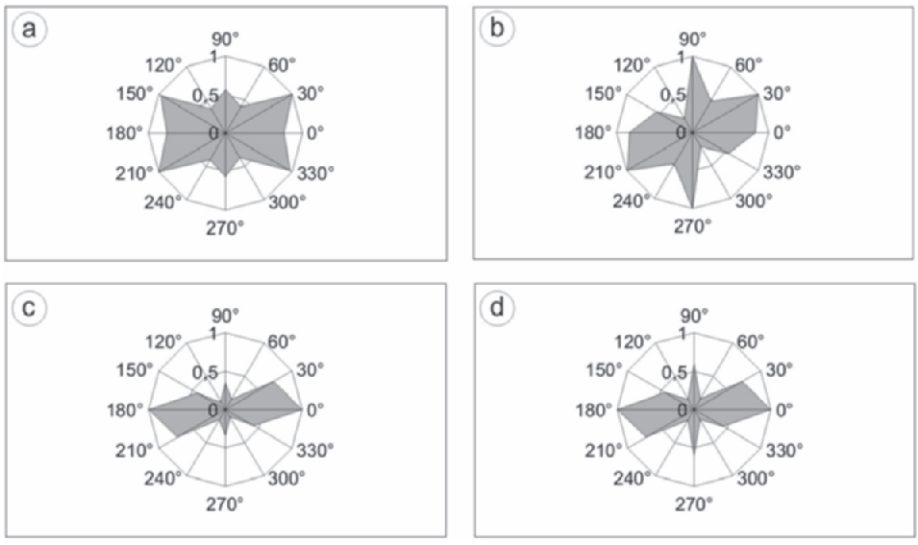

Figure 4. Roses of directions obtained from several images of granite from *Infante Don Luis* Palace. Angles are measured considering 0º the burnt surface.

the different types of fissures, though intergranular ones are slightly more abundant. The ratio intergranular/intragranular fissures is around 1.6. Burnt areas present an intense increase of the relative proportion of intragranular fissures. The values of the ratio intergranular/intragranular in this case is of the order of ~0.5.

4. CONCLUSIONS

Fire produces a noticeable mechanical decay in tough stones such as granite, as expected from other studies on natural stone materials. As it has been shown here, this decay is not only evident and measurable at the macro-scale but also at the micro-scale. As opposed to what is observed in granular stones, such as sandstones, in which predominant micro-effects generated by fire are related with mineralogical changes, in tough stones, such as the granite described in this paper, micro-effects of fire consist of the generation of new fissures and the growth of pre-existing ones. The process of fissuration of the studied burnt granites is circumscribed to the first 1.5 centimetres into the stone. Fire affects mainly the outer portion of rock, which even though it may not affect the bulk structural stability of the stone, it can have an outstanding impact on surface characteristics. Three types of fissures are found: intergranular, intragranular and transgranular. Transgranular fissures are sub-parallel to the material's surface and are found within the first half centimetre. In this outer area the temperature gradients are higher than in internal zones, both in terms of time and space, which promote a higher thermal stress enough for intragranular (and consequently transgranular) fissures to be formed. Transgranular fissures are the most important fissures to consider in decay processes such as spalling, as they form surfaces from which large fragments of the stone can detach. Inter and intragranular fissures can promote and enhance other decay processes such as granular disaggregation.

Transgranular, intragranular and intergranular fissures disappear progressively in this sequence as long one goes deeper following a longitudinal profile through the stone sections. The low conductivity of granite favours that the temperature gradients enough to promote fissuration during the fire event do not go deep within the stone and therefore no significant differences between burnt and un-burnt specimens are found deeper than 1.5 cm.

Three mechanisms of generation of fissures are observed: widening of pre-existing fissures, propagation of pre-existing fissures and nucleation of new fissures. The first mechanism to develop is the widening of pre-existing fissures, as it needs lower stress energy to be produced. Triple junctions of crystals are the most common areas where this mechanism takes place. New fissures develop mainly at the crystalline boundaries or are nucleated from

crystalline 'defects', such as exfoliation planes, inclusions or previous micro-fissures.

Microscopic techniques and image processing and analysis techniques have been marked out as a highly suitable technique for studying micro-effects generated by fire in historic buildings, as far as they can be carried out in small samples, compatible with the size of samples that should be obtained from heritage buildings.

Best results are obtained with images from microscopic techniques which offer high contrast images or binary images, such as Scanning Electron Microscopy in Backscattered mode (SEM-BS) and Fluorescence Microscopy.

Parameters obtained from the image treatment are indicative of the state of 'micro-decay' and could be used to be extrapolated or correlated to the results obtained for the bulk stone decay.

The results obtained so far have demonstrated the usefulness of image processing and analysis techniques as a non-destructive and complementary tool to help establishing, in a qualitative and quantitative way, the fracture system pattern resulting from mechanical stresses induced by fire.

ACKNOWLEDGEMENTS

The authors want to acknowledge the assistance of the Luis Brú Electronic Microscopy Centre of the Universidad Complutense and also the technical support of E.M. Pérez-Monserrat during this work. The Spanish Ministry of Education and Science is also acknowledged for a Research Contract *Ramón y Cajal* (MAdeB).

This work was partially supported by FCT sub-project DECASTONE of the Centre of Petrology and Geochemistry, IST, Lisbon, Portugal and the project MATERNAS of the regional government of Madrid

REFERENCES

Aires-Barros, L. Maurício, A. and Figueiredo, C., 1991, Experimental correlation between alterability indexes obtained by laboratorial ageing tests and by image analysis, in: *Proceedings of the Int. Conf. on La Détérioration des Materiaux de Construction*, La Rochelle, France, pp. 199-208.

Aires-Barros, L. Maurício, A. and Figueiredo, C., 1994. Profilometer and image analysis applications to "in-situ" study of stone decay phenomena, in: *Proceedings of the 3rd Int. Symp. on the Conservation of Monuments of the Mediterranean Basin*, Venice, Italy, pp. 19-24.

Allison, R.J. and Goudie, A.S., 1994. The effects of fire on rock weathering: An experimental study, in: *Rock Weathering and Landform Evolution*, D.A. Robinson and R.B.G. Williams eds., Wiley, Chichester, pp. 41-56.

Chakrabarti, B., Yates, T. and Lewry, A., 1996. Effect of fire damage on natural stonework in buildings. Construction and Building Materials, 10(7): 539-544.

COST-C17, 2001. Memorandum of Understanding for the implementation of a European Concerted Research Action designated as COST C17 "Built Heritage: Fire Loss to Historic Buildings", pp. 17.

Coster, M. and Chermant, J.L., 1985. Précis d'Analyse d'Images. Éditions du Centre National de la Recherche Scientifique, Paris, pp. 512.

Ehling, A. and Kohler, W., 2000. Fire damaged Natural Building Stones, in *Proceedings of 6th Int. Congress on Aplied Mineralogy ICAM*, Göttingen, pp. 975-978.

Figueiredo, C., Mauricio, A. and Aires-Barros, L., 1993. Rose of directions algorithm: an improvement of Nachet Ns 1500 implementation, in *Proceedings of the 5th Portuguese Conf. on Pattern Recognition*, RecPad'93, Porto, pp. 227-231.

Gómez-Heras, M., Varas, M.J., Alvarez de Buergo, M. and Fort, R., 2004. Characterization of changes in matrix of sandstones affected by historical fires, in: *Proceedings of the 10th Int. Congress on Deterioration and Conservation of Stone*, D. Kwiatkowski and R. Löfvendahl, eds., Stockholm 2004, pp. 561-568.

Gómez-Heras, M., 2006. *Procesos y Formas de Deterioro Térmico en Piedra Natural del Patrimonio Arquitectónico*. Universidad Complutense de Madrid, Madrid, 339 pp.

Gonzalez, R.C. and Woods, R.E., 1993. *Digital Image Processing*. Addison-Wesley Publishing Company, New York, 716 pp.

Hajpál, M., 2002. Changes in Sandstones of Historical Monuments Exposed to Fire or High Temperature, *Fire Technology*, **38**(4):373-382.

Hajpál, M. and Török, A., 2004. Mineralogical and colour changes of quartz sandstones by heat, *Environmental Geology*, **46**:311-322.

Mauricio, A. and Figueiredo, C., 2000. Texture Analysis of grey-tone images by mathematical morphology: a non-destructive tool for the quantitative assesment of stone decay. *Mathematical Geology*, **32**(5):619-642.

Ortiz, P., Galán, E., Vázquez, M.A., Guerrero, M.A. and Ortiz, R., 2000. Comparación entre metodologías de levantamiento de mapas de alteración como herramienta de diagnosis, in: *Proceedings of the 5th Int. Symp. on the Protection and Conservation of the Cultural Heritage of the Mediterranean Cities*, Seville, Spain, pp. 188-191.

Serra, J., 1982. Image Analysis and Mathematical Morphology. Acad. Press Inc., London, pp. 610.

Zezza, F. 1989. Computerised analysis of stone decay in monuments, in: *Proceedings of the 1st Int. Symp. for the Conservation of Monuments in the Mediterranean Basin*, Italy, pp. 163-184.